An observational and numerical study of the effects of the late sea breeze on ozone distributions in the Busan metropolitan area, Korea

In-Bo Oh, Yoo-Keun Kim[*], Hwa woon Lee, Cheol-Hee Kim

Department of Atmospheric Sciences, Pusan National University, Busan, Korea

Abstract

The late sea breeze (LSB), defined as a sea breeze with an onset time later than 1200 LST, and its impact on O_3 concentration distributions have been investigated both observationally and numerically over the Busan metropolitan area in Korea. The observed LSB mostly occurred under weak offshore synoptic flows during mid-day, and was found with late but apparent transitions in wind direction along with lower wind speed. The observed O_3 concentrations associated with the LSB demonstrated more significant enhancement of maximum O_3 concentrations than those of the early sea breeze by a factor of approximately 1.5. The main meteorological feature associated with the LSB was also reproduced by MM5 for typical cases. The numerically derived backward trajectories suggested that the increase of O_3 at the coastal site is mainly due to recirculated polluted air mass. The numerical simulation of O_3 concentrations from MM5/UAM-V shows that offshore winds of northwesterly synoptic flow swept the precursors of O_3 that were emitted by the urban area toward the sea during the early morning. As the development of the LSB was suppressed by the synoptic flow, a large near-stagnant wind field formed over the sea with intense photochemical activity at mid-day. However, the subsequent LSB with low wind speed was simulated in order to slowly re-advect the photochemically produced air parcels toward the inland area, resulting in both a significant enhancement of O_3 concentrations and high concentrations over the coastal area lasting for relatively longer hours. This result implies that the LSB plays an important role in the recirculation/accumulation of O_3 concentrations over the Busan metropolitan area, Korea.
© 2005 Elsevier Ltd. All rights reserved.

Keywords: Late sea breeze; Ozone distribution; Synoptic flow; MM5/UAM-V; Recirculation

1. Introduction

It is well known that the sea breeze has a significant effect on high ozone (O_3) concentrations in large coastal cities. The dynamic effects of the sea breeze associated with urban-scale transport and accumulation of O_3 including its precursors have been revealed to play a very important role in high O_3 occurrences. In previous studies, the major dynamic effects of the sea breeze have been speculated as being: (1) a formation of a temporal stagnant environment during the morning hours before the sea breeze develops (Blumenthal et al., 1978; Liu et al., 1990); (2) a convergence combined with terrain effects (Wang et al., 2001; Boucouvala

---

*Corresponding author.

E-mail address: kimyk@pusan.ac.kr (Y.-K. Kim).

et al., 2003); and (3) a recirculation of polluted air mass loaded with O_3 (Lalas et al., 1983; Uno et al., 1984; Hurley and Manins, 1995; Liu et al., 2002).

These dynamic effects have been associated with the onset time of the sea breeze. Previous studies have shown that the timing of the evolution of the sea breeze under different synoptic flows plays an important role in the transport and accumulation of O_3 and its precursors. For example, Kallos et al. (1993) and Blumenthal et al. (1978) pointed out that the late onset of sea-breeze-induced stagnant conditions in the morning, allowing pollutant concentrations to build up and enhancing O_3 accumulation in the afternoon. Ma Yimin and Lyons (2003) have shown that the interaction between the late sea breeze (LSB) and the synoptic scale trough is closely associated with the recirculation of coastal urban air pollution, and, as a consequence, brings higher O_3 episodes to coastal and inland areas. Recently, Ding et al. (2004) confirmed that the delayed sea breeze due to offshore synoptic winds can contribute to the daytime transport of pollution and high O_3 on the coast.

Although previous studies have suggested the importance of understanding the timing of the sea breeze related to O_3 transport and accumulation in coastal areas, they have tended to be observational studies or analysis of the trajectories of wind fields for particular episodes without photochemical modeling. Therefore, it is worth analyzing both observationally and numerically the quantitative onset time of the sea breeze and its contribution to O_3 concentrations.

The purpose of this research is to examine in a quantitative manner the variations of the onset time of the sea breeze over the Busan metropolitan area (BMA) in Korea. The LSB (with an onset time after 1200 LST) and its impact on high O_3 concentrations in the BMA were analyzed. The LSB and the early sea breeze (ESB) associated with O_3 concentrations are observationally contrasted, and the wind fields with trajectories were numerically studied by employing a meteorological model (MM5) for typical LSB cases. Finally the detailed structure of the LSB and its influence on the transport/accumulation of O_3 concentrations on 24 August 2001 were simulated by using coupled MM5 and a three-dimensional photochemical Urban Airshed Model (UAM-V).

2. Study area

Busan, the second largest city in Korea, is located on the southeastern tip of the Korean Peninsula (Fig. 1), with an area of $760 \, km^2$ and a population of approximately 4 million. Busan has a complex terrain including an irregular coastline and moderately high ($< 1 \, km$ above sea level) mountains. The urban center (BC in Fig. 1) is situated in a valley approximately $4 \, km$ away from the coastline; the valley floor is covered with tall buildings and roads. Since the early 1990s, Busan has rapidly urbanized and industrialized; as a result, the city has experienced a substantial increase in surface O_3 concentrations (Oh and Kim, 2002).

The prevailing synoptic winds over the BMA are generally northwesterlies in winter and southwesterlies in summer. During the warm season (i.e., from April to September), a well-developed land-sea breeze is a prominent feature, emerging under weak synoptic conditions. In accordance with the urban climate of the BMA, high O_3 concentrations in excess of 1-h/100 ppb, the Korean ambient O_3 quality standard, have frequently been observed.

The BMA has various pollutant emission sources such as vehicles, industrial facilities, ships and urban activity; the high emission lies over the downtown area located about $4 \, km$ from the coastline as well as the industrialized area in the southwestern BMA (see Fig. 2). Total annual emissions of approximately 51,800 tons of NO_2 and 34,000 tons of VOCs from point, line and area sources have been reported in the BMA (MOE, 2003), and a large part of these emissions (45% of NO_x, 20% of VOCs, respectively) were estimated to stem from the heavy traffic: there are approximately 862,000 registered vehicles. This vehicle density implies that the air in the BMA is highly polluted related to potentially high O_3 concentrations.

3. Method

3.1. Data sets

Both meteorological measurements obtained near the shore and O_3 concentrations measured by ground-based instruments from April to September over the period 1998–2002 (901 days) were used. Meteorological variables such as wind speed/direction and temperature were observed at the P5 site (an altitude of $20 \, m$ above ground level) located nearest to the sea, indicating a good site location to examine the characteristics of the air mass moving from sea to urban center with no topographical effect.

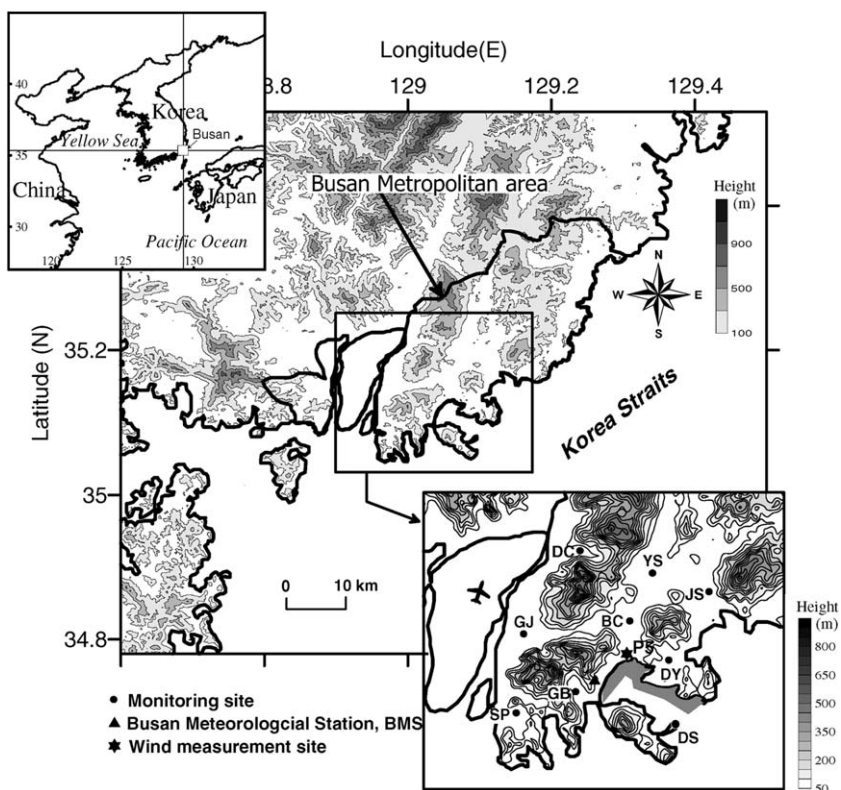We obtained the wind speed/direction and temperature averaged over 10 min from an anemometer

Fig. 1. Topographic map of the Busan metropolitan area in the southeastern Korea and the location of observation sites. The shaded area in bottom panel indicates the Port of Busan.

(Model 05103) and thermometer (Model HMP45C), made by the Campbell Scientific Company, USA, installed at P5. The observation error ranges of wind direction, wind speed, and temperature were $\pm 0.3°$, $\pm 0.3 \, \mathrm{m\,s^{-1}}$, and $\pm 0.2°$ (at $20°$), respectively. Other meteorological data such as solar radiation, precipitation and cloud cover were collected from a Busan meteorological station (BMS) located halfway up the hill about 4 km SW of P5. Hourly O_3 concentration data were gathered from nine monitoring sites (see Fig. 1) operated by the Korean Ministry of Environment (MOE). The O_3 monitors were made by Dasibi (model AH-1003), which utilizes U.V. absorption and are accurate to 2–4 ppb. Other pollutants such as NO_2 and CO data obtained at the DS monitoring site were also used to analyze the movement of polluted air and the photochemical process.

3.2. ESB and LSB and their onset times

Sea breeze is caused by the temperature differences between the hot land and the cool sea (Simpson, 1994). However, its development and evolution can be influenced by various factors such as background synoptic flows (Bechtold et al., 1991; Zhong and Takle, 1993; Ma Yimin and Lyons, 2000), complex coastlines, rugged hills and other mountain effects (Pielke, 1974; Kikuchi et al., 1981; Abbs and Physick, 1992). Therefore, for an observational approach in exploring the timing of the LSB evolutions, it is necessary to define the sea-breeze day considering both thermally induced pure sea breeze and background synoptic flows.

Based on the surface meteorological variables obtained at P5, the sea-breeze day was defined in this study as a clear day when the wind direction was confined to southeasterly or southerly (90–225°), and a wind speed of more than $2 \, \mathrm{m\,s^{-1}}$ was maintained for at least 4 h during the daytime. The onset time of the sea breeze was also defined as the time when the onshore wind (the southeasterly or southerly wind) starts to blow with a wind speed of at least $2 \, \mathrm{m\,s^{-1}}$ at P5 soon after an instantaneous change in wind direction or wind speed ($< 2 \, \mathrm{m\,s^{-1}}$). In identifying the characteristics of the observed O_3

concentrations in association with the onset of the sea breeze, in detail, we subdivided the sea-breeze days into three categories: (1) ESB days, which have an onset time before 0900 LST; (2) normal sea-breeze (NSB) days, with an onset time between 1000 and 1100 LST; (3) LSB days with an onset time after 1200 LST.

3.3. Modeling for LSB and ozone concentrations

In order to simulate the LSB, the fifth generation of the mesoscale model (MM5, Dudhia et al., 2004) was employed. The horizontal resolutions of the nested domain here were 54, 18, 6, and 2 km, respectively; 20 vertical sigma layers were specified with higher resolution near the ground (about 13 layers below 3 km above ground level) and the top layer of 200 hPa. Six-hourly NCEP (National Centers for Environmental Prediction) global analysis data, with a horizontal resolution of $2.5°$ in latitude and longitude, were used to obtain the initial and boundary conditions for the MM5. The explicit moisture scheme for mixed-phase, the radiation scheme of rapid radiative transfer model (RRTM), and the surface scheme for multi-layer soil thermal diffusion were adopted and the planetary boundary layer (PBL) was parameterized using the MRF-PBL. US geographic survey data were used to obtain the land use (Dudhia et al., 2004).

To simulate the temporal and spatial O_3 distribution by LSB for 24 August 2001, we employed the three-dimensional photochemical Urban Airshed Model with a variable grid (UAM-V, version 1.30) developed by System Applications International (SAI). The UAM-V is designed to simulate the concentrations of both inert and chemically reactive pollutants by considering the physical and chemical processes in the atmosphere. This model incorporates horizontal and vertical multiple grid nesting, a plume-in-grid treatment of elevated point source emission, and three-dimensional meteorological inputs (SAI, 1999). The chemical process employs an extended version of Carbon Bond Mechanism IV (CB-IV), containing over 90 reactions and over 30 chemical species.

The UAM-V domain is composed of 50×50 regular horizontal grids (2 km resolution), covering southeastern Korea. The eight vertical sigma layers ($\sigma = 0.998, 0.970, 0.945, 0.900, 0.850, 0.805, 0.740,$ and 0.675) from MM5 output below 3 km were used. All of the required meteorological input variables such as wind, temperature, water vapor,
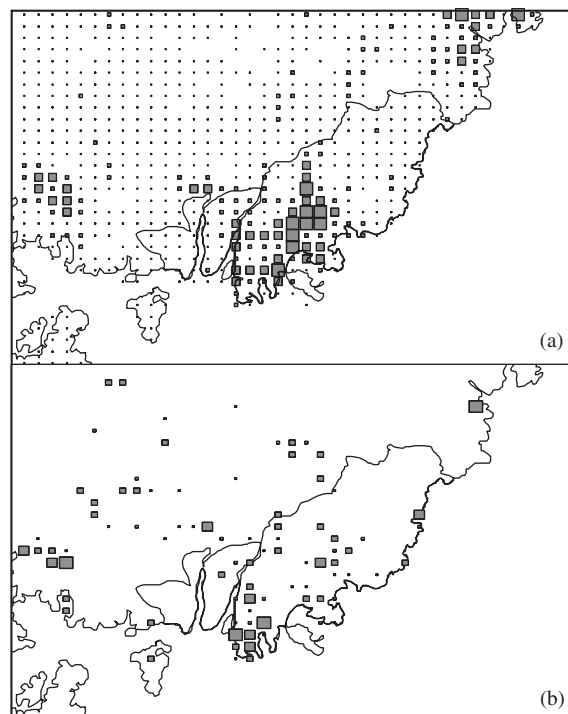

Fig. 2. Horizontal distributions of NO_x emission from (a) area/line and (b) point sources. The size of shaded rectangles is proportional to the emission amount (The largest emission rate is 32 and 55 kg h^{-1} for area/line and point sources, respectively).

vertical turbulent exchange coefficient and height/pressure were extracted from the finest domain (2 km) of MM5.

The disaggregated emission inventory with high spatial (2×2 km) and temporal (1 h) resolution made by BMC (Busan Metropolitan City) (2002) was used. All emission sources including area, line, and point sources were aggregated into the 2×2 km UAM-V grid, and hourly emission rates of inorganic species (NO_x, CO, and SO_2) and 20 classes of VOCs were assigned to each grid location. The distribution of total NO_x emissions from area/line and point sources in the model domain are shown in Fig. 2. Since reliable data for VOCs are still lacking over the BMA, the scaled VOC emission of the previous study (Kim et al., 2003) was applied. This emission was derived by the test in comparison of the predicted and observed concentrations. As a result, we increased total VOC emissions by a factor of approximately 2.5 over the whole BMA.

The initial surface concentrations of O_3, CO, NO_2, and SO_2 were horizontally interpolated from available measured values obtained from the monitoring

Table 1
Surface meteorological conditions associated with the evolution of the sea breeze for different sea-breeze days during April–September 1998–2002

Category	Number of days	Sunrise time (LST ± min)	Daily solar radiation (MJ m^{-1})	Daily max. T (°C)
ESB days	48	0527 ± 17	22.5 ± 2.6	24.8 ± 4.4
NSB days	133	0535 ± 22	21.3 ± 3.5	23.2 ± 4.6
LSB days	57	0536 ± 23	21.0 ± 3.7	25.3 ± 4.4

sites. The initial concentrations at higher levels were set to background concentrations except for the O_3 concentrations. For the O_3 concentrations, the averaged values obtained by ozonesonde measurements during the summer of 2001 were used (BMC, 2002). The UAM-V simulation was conducted for 72 successive hours for the episode day including the previous 2 days. The first 24 h served as a model spin-up period in order to minimize the influence of insufficient initial conditions. For the boundary conditions, we assumed O_3 and other pollutants to be constant values in a clean and remote atmosphere (Chang and Cardelino, 2000).

4. Observational features

4.1. Comparison between ESB and LSB

In accordance with the prescribed standards, the frequency of sea-breeze days was found to be around 33% (301 days) of the total 901 days with the onset times of between 0800 and 1500 LST. Of the total sea-breeze days, ESB, NSB, and LSB days were determined to occur approximately 20% (48 days), 56% (133 days), and 24% (57 days), respectively. The instances of undetected onset time of sea breeze (63 days) were discarded for the calculation.

Table 1 shows the sunrise times, daily incoming solar radiation and daily maximum temperatures for the ESB, NSB and LSB days, respectively. It is of great interest to note that, for all three categories of days, there are no appreciable differences in either sunrise times or incoming solar radiation which are the primary factors in the development of thermally induced sea breeze circulation. This clearly indicates that differences in sea breeze timing can be caused by differential external forces of background synoptic winds (Helmis et al., 1995). In Fig. 3c, the relatively strong winds during early to mid-day for the ESB days compared to the LSB days demonstrate well the different synoptic forces
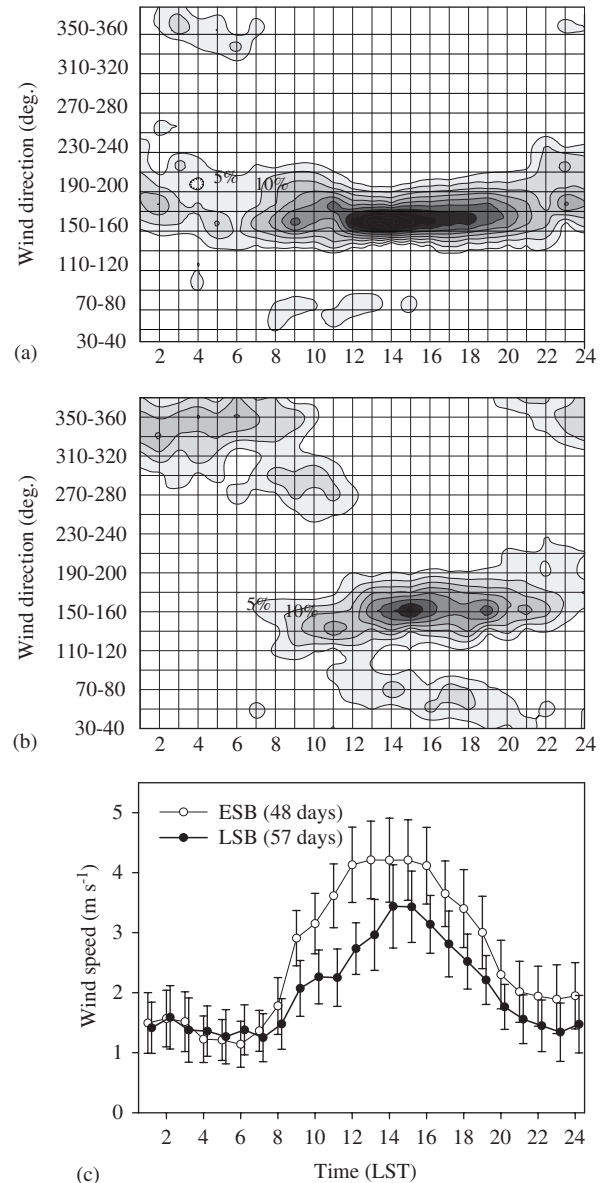

Fig. 3. Diurnal variations of frequency of wind direction for (a) the ESB days, (b) the LSB days, and (c) the averaged wind speeds for the ESB and LSB days at P5 during April–September 1998–2002. Error bars in (c) represent one standard deviation.

Table 2
Synoptic conditions for the different sea-breeze days

Category	Dominant 850 hPa pressure pattern	Major 850 hPa flow over BMA
ESB days	Ridge of North Pacific or Okhotsk High is extending to Korean peninsula (65%)	South-southeasterly (average wind speed = 7.7 m s^{-1})
NSB days	Weak high-pressure systems are located over the Korean peninsula (75%)	—
LSB days	Low pressure is located over northeastern China with weak trough extending southward, or high pressure is located over Yellow Sea with ridge influencing Korea peninsula (74%)	Weak north-northwesterly (average wind speed = 5.6 m s^{-1})

Table 3
The observed O$_3$ concentrations for the different sea-breeze days

Category	Daily max. 1-h O$_3$ (ppb)	Number of days $\geqslant$1-h/ 100 ppb[a]	Daily max. 8-h O$_3$ (ppb)	Number of days $\geqslant$8-h/ 60 ppb[a]
ESB days	49.2 ± 13.8	2 (4.2)	39.3 ± 11.2	18 (37.5)
NSB days	56.6 ± 13.6	14 (10.5)	45.2 ± 10.8	64 (48.1)
LSB days	70.4 ± 14.8	17 (29.8)	55.8 ± 11.8	46 (80.7)

[a]The values in parenthesis indicate the probability of O$_3$ exceedances. 100 and 60 ppb are the Korean ambient 1- and 8-h O$_3$ quality standard, respectively.

affecting the evolution of the sea breeze (Pielke, 2002). The synoptic maps of 850 hPa level revealed also that onshore (southerly or southeasterly) synoptic flows were prevalent during ESB days (80% occurrence), while weak offshore (northerly or northwesterly) synoptic flows were dominant during LSB days (74% occurrence). Table 2 summarizes the dominant synoptic conditions for ESB and LSB days.

It is also interesting to note that the daily maximum temperature does not correlate well with the onset of sea breeze (Table 1). In recognition that solar radiation and temperature are believed to be very important meteorological factors in determining photochemical O$_3$ production, there have been nearly no differences in the potentials for photochemical formation during the three categories of days given the prominent observed differences in O$_3$ levels between ESB and LSB days, indicating the importance of the dynamic effects of the atmosphere.

Fig. 3 shows the diurnal variations of wind direction and average wind speed for ESB and LSB days, respectively. For both types of days, southeasterly winds dominated in the afternoon. However, lower wind speeds were favored under the LSB condition with a shift in wind direction

toward northerlies during mid-day. As shown in Fig. 3c, for the LSB days, the maximum wind speed has a time lag of 1–2 h delay in response to the synoptic flows, resulting in relatively lower daytime wind speeds than those on the ESB days. This lag is believed to have an important bearing on the different air pollution concentration distributions.

4.2. Ozone distributions associated with the onset of sea breeze

Table 3 summarizes the daily maximum 1- and 8-h averaged O$_3$ concentrations as well as the frequencies of high O$_3$ days obtained at the nine monitoring sites during April–September 1998–2002. A high O$_3$ day is defined as a day when O$_3$ concentrations were observed to exceed the Korean standard level (1-h/100 ppb, 8-h/60 ppb) at least at one of the nine sites. For LSB days, the O$_3$ levels and the frequency of high O$_3$ days are clearly higher than those for the ESB or NSB days. As in Table 3, the probabilities of high O$_3$ occurrences are found on the LSB days, reaching up to 29.8% (1-h) and 80.7% (8-h), respectively. Every statistic from the O$_3$ observations exhibited an increased O$_3$ level

with the retarded onset of the sea breeze under the same potential of photochemical production as inferred in Table 1. This result also suggests the importance of the dynamic effects of accumulation and transport of O_3 concentrations where the meteorological phenomena of the LSB, such as the late but distinct wind change with low wind speed, can be responsible for high O_3 concentrations in coastal areas, as illustrated in Fig. 3.

This implication is more obvious in Fig. 4, where the diurnal variations of O_3 concentrations averaged over the nine sites for both the ESB and LSB days are depicted. There are nearly no differences between ESB and LSB days with low level O_3 (~20 ppb) until 1000 LST due to titration of O_3 by urban NO emission ($NO + O_3 = NO_2 + O_2$). After 1000 LST, however, the observed maximum O_3 concentration on the LSB days is approximately 50% higher than on ESB days, and the maximum

O_3 occurrence on LSB days lagged behind those on ESB days by about 2 h, which represents the O_3 accumulated by weak wind conditions and transported by the subsequent LSB. Likewise, large differences in O_3 concentrations between the ESB and LSB days during the mid to late afternoon can be mainly attributed to the high level O_3 transported by LSB.

Fig. 5 shows the diurnal variations of O_3, NO_2 and CO concentrations observed at the coastal DS site. DS is the observation site located at the upstream area of the sea breeze and not generally influenced by the urban emissions. On LSB days, the O_3 concentrations at night and the early morning show low levels; however, there is a marked increase in the early morning hours starting at 0800 LST with a maximum around 1500 LST in the afternoon, consequently showing higher levels than on ESB days after 1200 LST. With lower O_3 concentration, higher NO_2 and CO concentrations from night to early day suggest that the polluted air emitted from the urban area is swept out toward the sea by offshore winds; furthermore, urban air pollutants with loaded O_3 concentrations can possibly be re-advected from the ocean by LSB during mid-day. The higher concentrations of NO_2 and CO on LSB days compared to those on ESB days throughout the day indicate a higher potential for photochemical O_3 production and are also thought to be due to the influence of urban pollution and its recirculation, showing agreement with previous studies (Wang et al., 1998).

5. Numerical modeling of LSB and its impact on ozone distribution

In order to ensure the dynamic effects associated with LSB on high O_3 concentrations, we selected
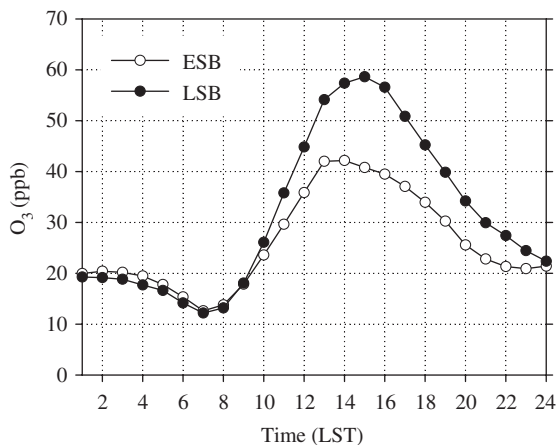

Fig. 4. Diurnal variation of average O_3 concentrations observed at nine sites for the ESB and LSB days during April–September 1998–2002.
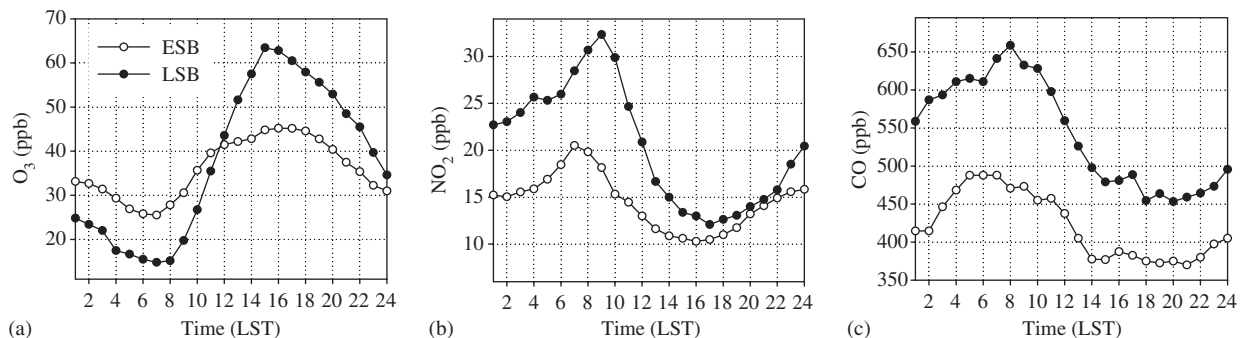

Fig. 5. Diurnal variations of average (a) O_3, (b) NO_2 and (c) CO concentrations observed at DS for the ESB and LSB days during April–September 1998–2002.

typical LSB cases with high O_3 concentrations during the study period. Meteorological modeling was conducted using MM5 for all selected cases for generating three-dimensional wind fields, and trajectories were analyzed in association with observed O_3 concentrations. Also, the results of the features of LSB and O_3 concentration distributions on 24 August 2003 derived by employing the coupled MM5/UAM-V are discussed in detail.

5.1. Case studies for typical LSB with high O_3 concentrations

Of the 57 LSB days, the four cases with the highest levels of daily maximum O_3 were selected. Table 4 shows the meteorological conditions and O_3 concentration levels for those four cases. For those cases, the BMA was predominantly influenced by

the north to northwesterly synoptic flow in cyclonic (trough) or anticyclonic (ridge) curvature, leading to a retarded sea breeze development. Under these conditions of offshore synoptic flow and favorable photochemical conditions with daily maximum temperatures over 25 °C, LSB was clearly observed with high O_3 concentrations in the BMA. Particularly, higher O_3 concentrations for most cases (except for case 4) were observed at coastal sites (GB, DY, DS) with lower NO_x emissions (see Fig. 2). This implies the importance of the recirculation of O_3 laden air mass.

In order to identify the features of LSB and its resultant recirculation phenomena, MM5 was employed for the selected four cases. Fig. 6 shows the simulated and observed time series of wind direction/speed at P5. Although there are some differences between the simulated and observed winds,

Table 4
Summary of the selected four LSB cases during April–September, 1998–2002

Case no.	Date (day/month/yr)	Dominant synoptic flow on 850 hPa	Daily max. T (°C)	Daily max. 1-h O_3 (ppb)[a]	O_3 con. (ppb) and sites $\geqslant$1-h/100 ppb
Case 1	15/9/1998	NW (trough)	29.6	86.0 (50.8)	111(GB)
Case 2	19/9/2000	NE (ridge)	25.0	92.3 (54.5)	123 (GB), 104 (DS), 111 (BC), 104 (DY)
Case 3	24/8/2001	NW (trough)	31.4	100.3 (46.6)	128 (DY), 120 (YS), 114 (BC), 114 (DC), 112 (DS), 111 (JS)
Case 4	21/5/2002	NW (ridge)	27.4	81.9 (56.8)	102 (DC)

[a]Average values over the nine sites. Values in parentheses indicate the respective monthly averages.
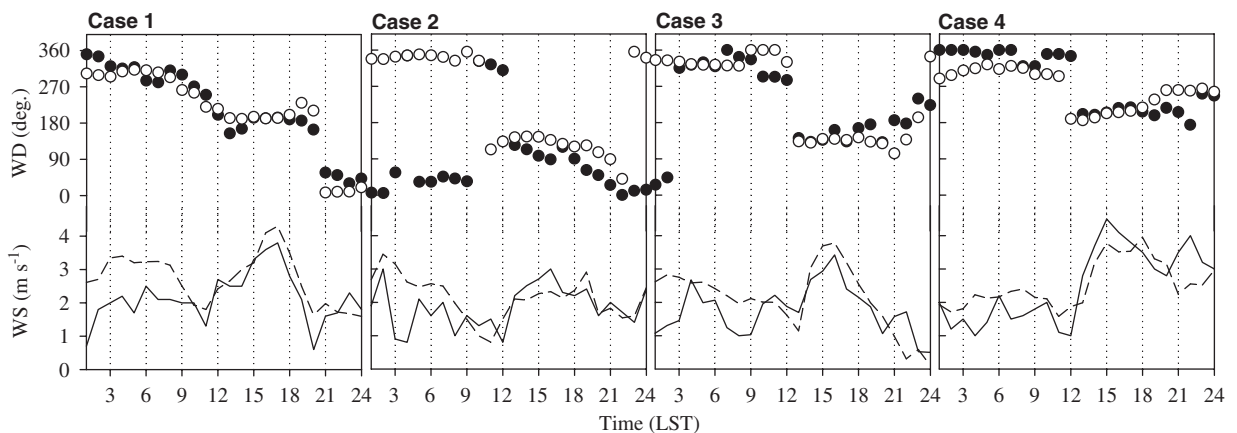

Fig. 6. Diurnal variation of observed (dots and solid lines) and simulated (open circles and dashed lines) winds at P5 for the selected four LSB cases.
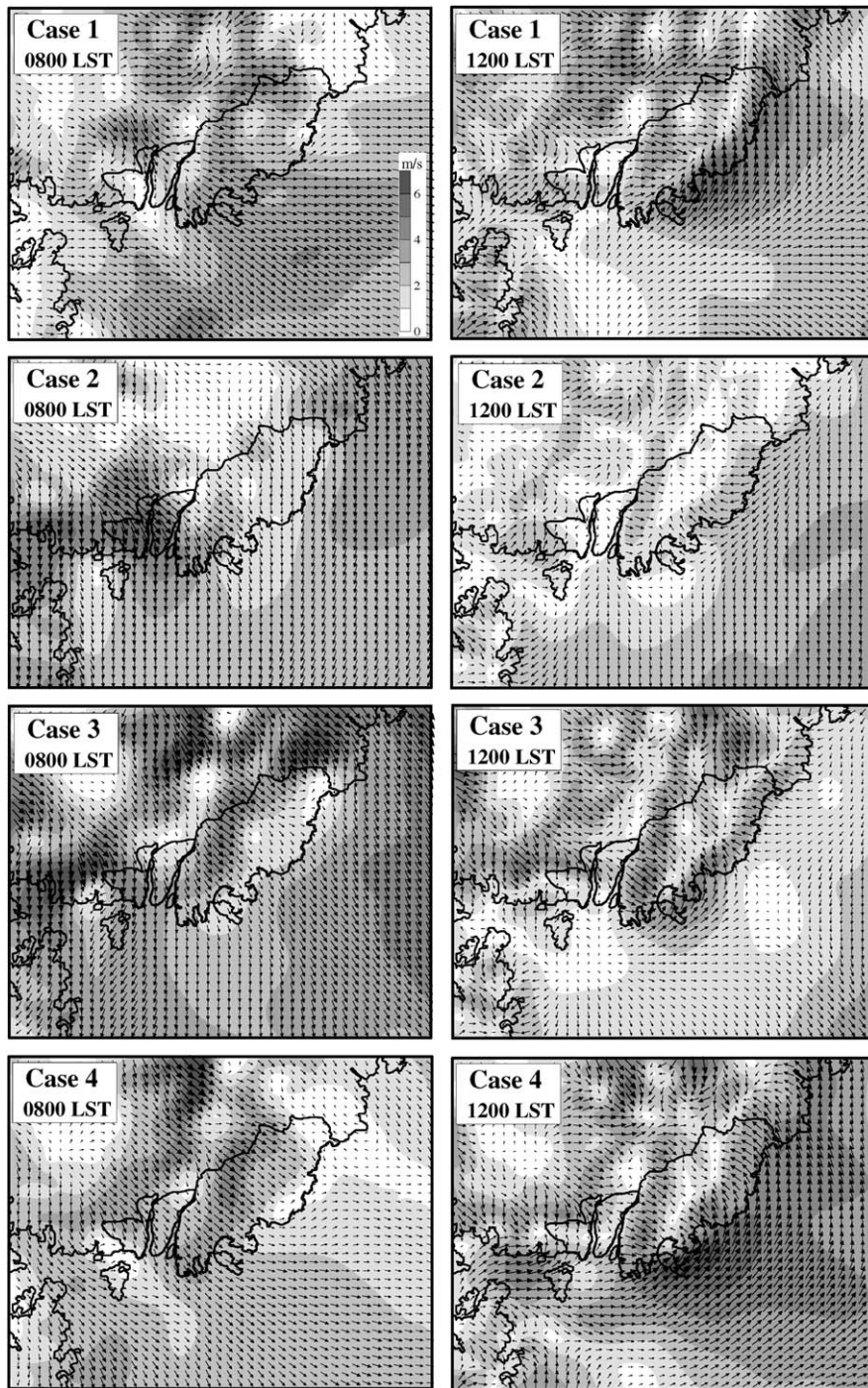
Fig. 7. Horizontal distributions of the simulated wind vectors at 0800 and 1200 LST for the selected four LSB cases. Shaded contour represents wind speed (m s^{-1}).

overall the model reproduced the diurnal variations in winds with reasonable accuracy. Fig. 7 shows the simulated horizontal wind vectors at the lowest model level at 0800 LST and 1200 LST (the time before sea breeze arrives at P5). At 0800 LST,

offshore winds are dominant for the entire domain for all cases, implying that air pollutants were advected to downstream areas (the near ocean). As the LSB develops and begins to move inland at 1200 LST, a strong wind convergence zone forms along
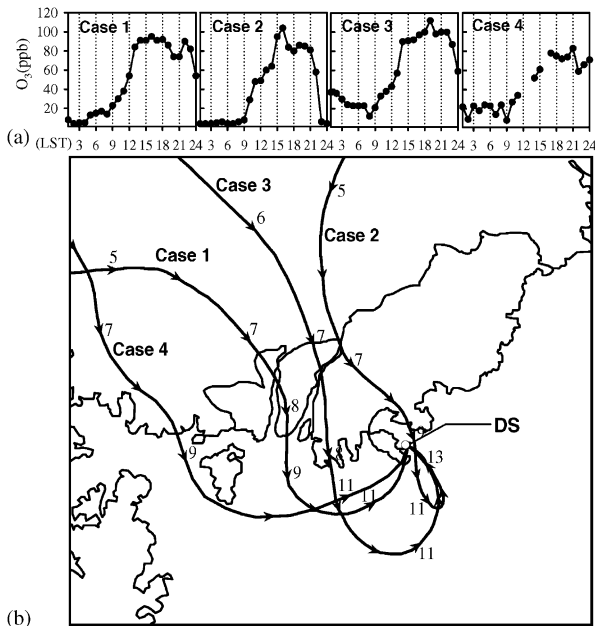
Fig. 8. (a) Diurnal variation of observed O_3 concentration at DS for the LSB cases and (b) backward trajectories arriving at DS at 1200 LST (case 1, 4), 1300 LST (case 3), 1400 LST (case 2). Numbers along the trajectories denote the hours (LST) for the selected four LSB cases.

the shoreline, which is clearly comparable to that of the NSB day under weak synoptic conditions (Lalas et al., 1987). As a result, a near stagnant condition is formed over the inland urban center and its surroundings, leading to an accumulation of O_3 and its precursors that can enhance O_3 concentration in the afternoon. Blumenthal et al. (1978) also suggested that the late onset of sea breeze allowed pollutant concentrations to build up in the stagnant air.

The recirculation of the urban plume can be clearly identified by backward trajectories calculated using MM5 outputs with a 2-km resolution. Fig. 8 shows the time variation of O_3 concentrations observed at DS and the trajectories of air masses arriving at DS at the time when O_3 concentrations started to increase rapidly with the development of LSB (case 1: 1200 LST, case 2: 1400 LST, case 3: 1300 LST, and case 4: 1200 LST). The calculated trajectories for all cases suggest that inland air masses might have arrived at DS, traveling over the sea before returning back to the land. These air masses resided over the sea for at least 3 h around mid-day before returning to the shore. For cases 2 and 3, the recirculation of polluted air masses passing over the area of high NO_x emissions in the

BMA (see Fig. 2) can be the main reason for the rapid increase in O_3 concentrations for 1400–1500 LST (case 2) and 1300–1400 LST (case 3), and relatively higher maximum O_3 levels compared to those of the other two cases. The trajectory pattern of case 3 shows that the polluted air mass traveled relatively farther away from the shore for a longer time unhindered by sources of fresh nitric oxide (NO) compared to those of the other three cases. This indicates that much of the O_3-rich air accumulated over the sea can be recirculated to the inland area, leading to higher and longer lasting O_3 concentrations at the coastal area.

5.2. Photochemical modeling on 24 August 2001

On 24 August 2001, the BMA was located in a cyclonic curvature under a weak trough extending from the northeast of the Korean Peninsula (Fig. 9a). The northwesterly offshore synoptic flow dominated the BMA, resulting in a typical LSB case. In addition, meteorological conditions (a clear sky and a high temperature of 31.4 °C) favorable to sea breeze formation and photochemical O_3 production were observed.

Fig. 9b and c show the diurnal variations of the wind direction/speed measured at P5, and O_3 concentrations observed at the three coastal sites (DS, DY, and JS) and one urban site (BC) on 24 August 2001. In the morning, northerlies or north-easterlies were monitored before the onset of the sea breeze, representing a typical meteorological condition in which urban air pollutants are steadily advected to the sea during the rush hour. With the incoming solar radiation flux striking the ground (sunrise at 0550 LST), a low wind speed was formed until the onset of the sea breeze. At 1200 LST, there is a sudden shift in wind direction from north-easterly to southeasterly and then a wind speed of more than $2.0 \, \mathrm{m \, s^{-1}}$ is observed after 1240 LST. In these circumstances, O_3 increased rapidly and high concentrations exceeding 100 ppb lasted until the early evening at all sites.

Fig. 10 shows the simulated and observed O_3 concentrations at two coastal sites (DS and DY) during 23–24 August. UAM-V captured well the rising O_3 concentration after 0900 LST due to mixing and formation, and the significant increase at the arrival of LSB, although there have been relatively large discrepancies between real and simulated concentrations in the evening hours. Overall, the model results compared well with the observations,
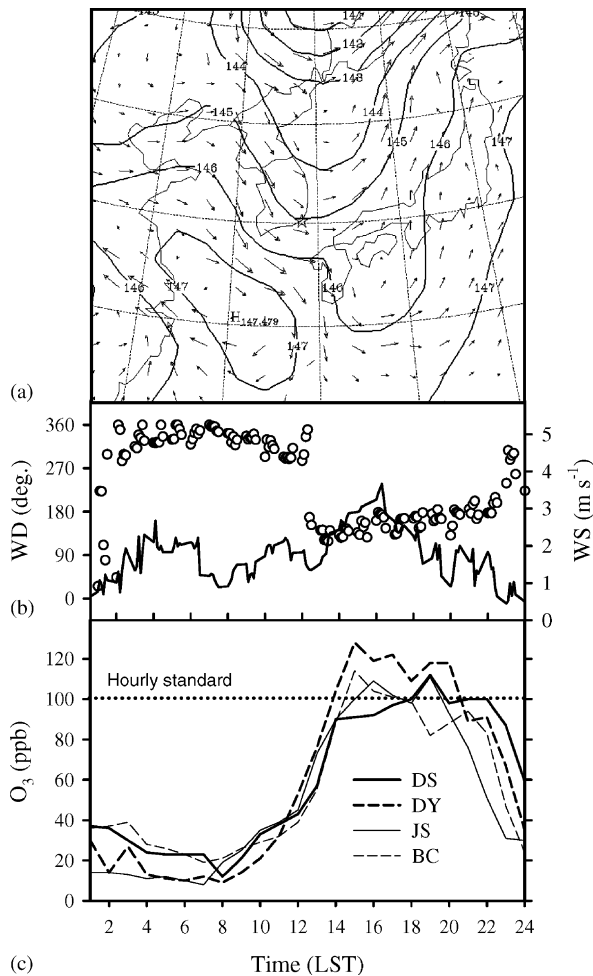
(a)

(b)

(c)

Fig. 9. (a) Horizontal distribution of geopotential height and wind vectors (maximum value indicates $17.5\,\mathrm{m\,s^{-1}}$) at the 850 hPa level at 0900 LST (from FNL ARLPLOT on NOAA's web site), (b) diurnal variations of observed wind direction/speed (in 10 min intervals) at P5, and (c) O_3 concentrations at four sites on 24 August 2001.

Fig. 10. Comparison between simulated and observed surface O_3 concentrations at DS and BS during 23–24 August 2004.

with an average correlation coefficient (r) of more than 0.7 ($p < 0.05$) over the nine monitoring sites for the entire simulation period; furthermore, all of the observation sites showed a very acceptable range of maximum O_3 concentrations.

Statistical analysis of the simulation and the observations were performed using US EPA-recommended measures (mean normalized bias error: MNBE, mean normalized gross error: MNGE, unpaired peak prediction accuracy: UPA) to evaluate the simulated O_3 concentrations (US EPA, 1991). These statistics were computed using observation-simulation pairs (cut-off level = 40 ppb) from all nine monitoring sites for the entire simulation period. The
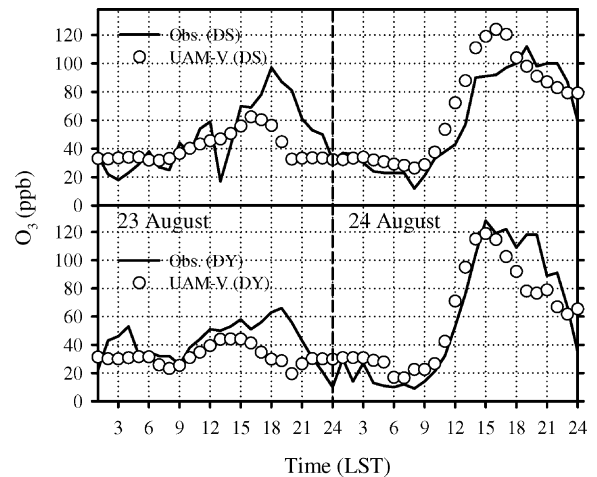
results showed values of -10%, 27% and 9% for MNBE, MNGE and UPA, respectively, which meet the US EPA-recommended criteria of ± 5–15%, 30–35%, and ± 15–20% for the respective statistics.

The simulated horizontal distributions of O_3 concentrations, as well as the wind fields at the lowest model level, are presented in Fig. 11. At 0800 LST, we can see a dominant northwesterly (off-shore) flow which can advect O_3 precursors emitted from the urban or industrial areas to the sea. The simulated O_3 concentrations over the sea adjacent to the coast of the BMA are very low, indicating the effect of chemical scavenging of O_3 caused by advected NO-enriched air from inland sources. This is in good agreement with observations at coastal sites (DS and DY) in Fig. 10.

At 1200, 1400 and 1600 LST, with the late development of onset of the sea breeze, high O_3 concentrations can clearly be seen over the sea in Figs. 11b–d. These are attributed to the photochemical O_3 production from the transported inland-polluted air that was unhindered by NO. At 1200 LST, O_3 concentrations increased over the sea under the strong insolation and penetrated inland as the LSB developed along the shoreline, suggesting the effect of recirculation of polluted air masses. These higher concentrations over the sea at this time were similarly simulated in Athens using a photochemical dispersion model (Moussiopoulos et al., 1955).

By 1400 LST, high O_3 concentrations are simulated over the coastal area extending to the remote sea area, which is due to both accumulation of transported O_3 by the LSB and the active
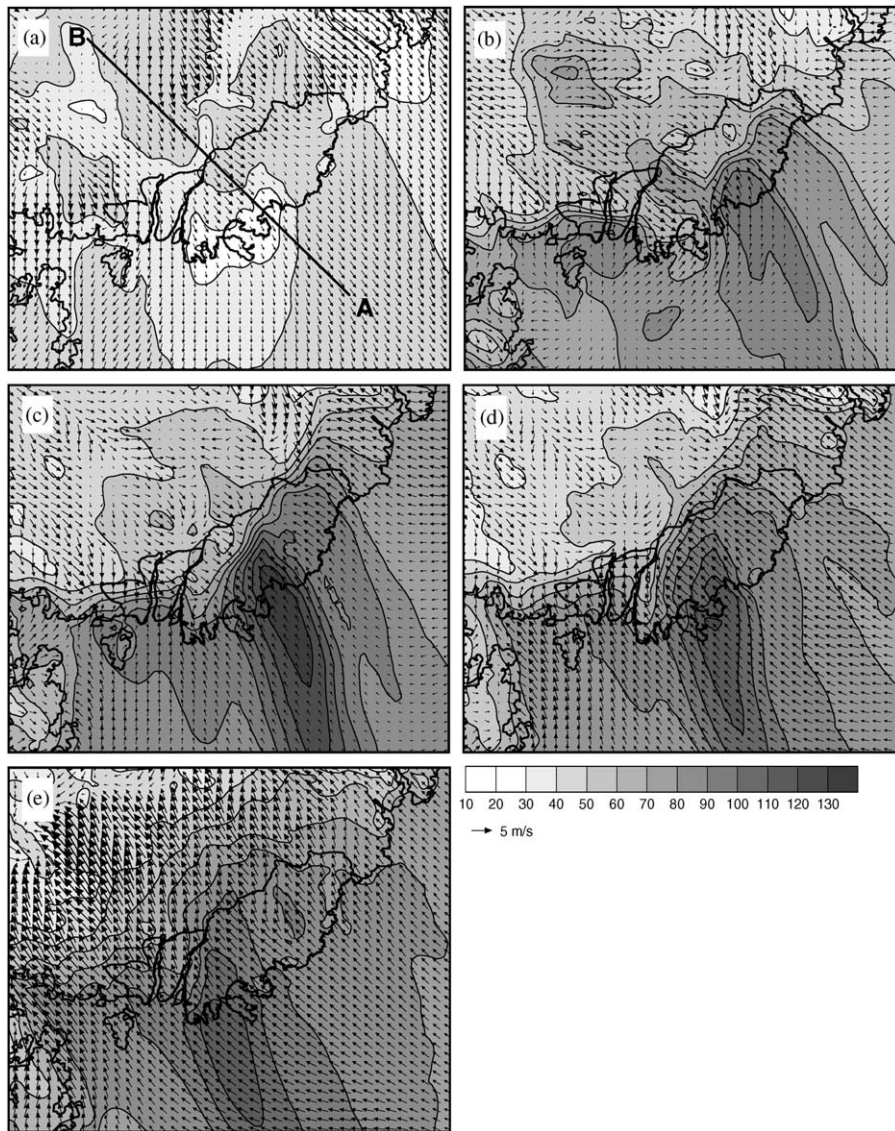
Fig. 11. Horizontal distributions of the simulated wind vectors and O_3 concentrations at (a) 0800 LST, (b) 1200 LST, (c) 1400 LST, (d) 1600 LST, and (e) 1800 LST on 24 August 2001. The thick line indicates the vertical cross-section from A [grid number (IX, IY) = (35, 14)] to B [(IX, IY) = (15, 37)]).

photochemical process. At 1600 LST, the area of elevated O_3 extended inland by the LSB, whereas the areas with O_3 levels over 90 ppb largely shrunk, mainly due to the advection of unpolluted marine air by the offshore propagation of the sea breeze. At 1800 LST, O_3 concentrations over the outer region of the BMA increased by inland penetration of the LSB.

Fig. 12 shows the vertical cross-section of both wind components and O_3 concentrations (A–B line indicated in Fig. 11) at 1200, 1400 and 1600 LST, respectively. The vertical values were calculated at

eight levels in the lowest 3 km above sea level. At 1200 LST, the sea breeze in the lower atmosphere was established near the coast. A stagnant condition was simulated over the sea approximately 10 km away from the coastline. This condition contributed to photochemical O_3 built up in the polluted air over the sea. At 1400 LST, however, as the offshore background flow continued to reduce the inland penetration of the sea breeze, the polluted air moved slowly toward the coastal area with an accumulating O_3 concentration. In particular, a heavily polluted O_3 layer simulated at around 700 m over the sea
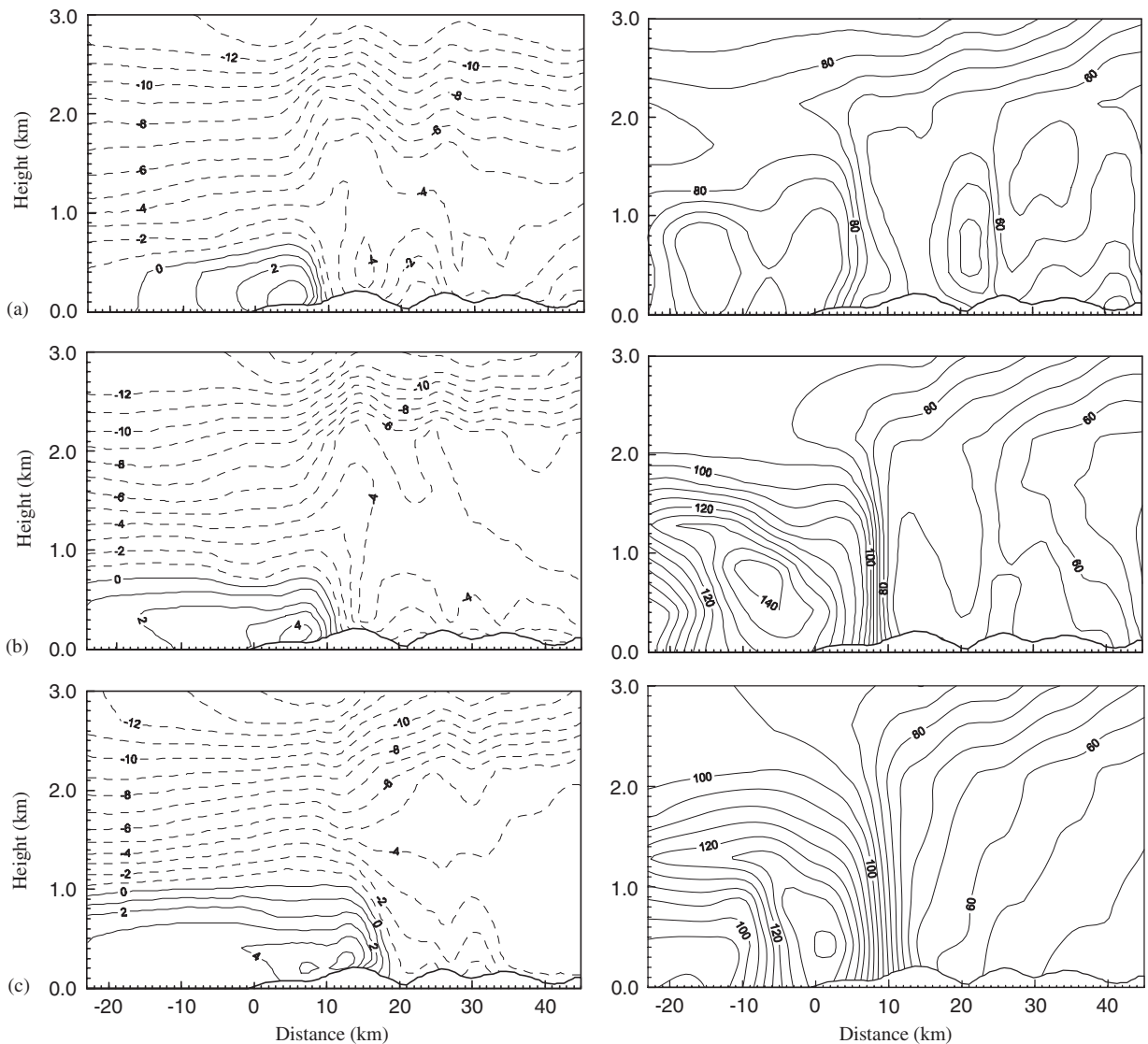
Fig. 12. Simulated vertical cross-shore contours of wind component (left, m s^{-1}) and O$_3$ (right, ppb) at (a) 1200 LST, (b) 1400 LST and (c) 1600 LST on 24 August 2002.

level was found. This finding is presumably due to the effect of aged pollutants trapped above the marine layer in stagnant air decoupled from the surface (Blumenthal et al., 1978). Measurements of elevated O$_3$ above a coastal area under sea breeze conditions were reported by Lalas et al. (1987) and Wakamatsu et al. (1999).

As LSB penetrates inland from the coastline, a high O$_3$ cell over the sea moves closer to the shore at 1600 LST. It is also of interest that high O$_3$ concentrations remained at around 1.2 km over the sea level due to the advection of O$_3$ concentra-

tions by the return flow, combined with a weak offshore synoptic flow.

In this simulation, LSB and its dynamic effects on high O$_3$ concentrations were successfully simulated by MM5/UAM-V, confirming the recirculation process of air pollution over the BMA. The pattern of pollution being emitted from the urban area, initially advected to the sea, built up over the sea, and subsequently transported by LSB to the coastal area in the late afternoon, was successfully simulated. Therefore, this recirculation of polluted air, together with local O$_3$ production under weak wind

conditions during early to mid-day, will play a significant role in the enhancement of the levels of O_3 concentration which are closely related to severe O_3 concentration episodes over the BMA.

6. Conclusions

Observational as well as numerical studies were conducted to investigate the impact of the late sea breeze (LSB) on the temporal and spatial distribution of O_3 concentrations over the Busan metropolitan area (BMA). The LSB has been observed mostly under the weak offshore synoptic flow, which plays a role in suppressing the development of the sea breeze; as a result, the inland penetration of the sea breeze was distinctly prolonged. The LSB phenomenon was also found to be closely associated with pronounced wind change and low wind speed over the coastal area during mid-day, resulting in higher O_3 concentration (O_3 statistics exhibited an increased O_3 level with the retarded onset of the sea breeze) and delaying the occurrence time of the maximum O_3 levels compared to early sea breeze cases.

The observational and numerical analysis of four typical LSB cases clearly demonstrated the enhanced O_3 concentration together with the meteorological features over both the sea (distinct change of wind direction) and coastal area (low wind speed) at mid-day. In addition, backward trajectories for the LSB cases suggested that coastal areas can be influenced by recirculated polluted air masses that originated from inland high emission areas.

The MM5/UAM-V model simulation confirmed the observed O_3 concentration distributions, and explained the prevailing main features of the LSB circulation in the conditions of a weak offshore synoptic flow. The simulated horizontal and vertical distributions of O_3 concentrations demonstrated that the LSB phenomenon plays a significant role in the accumulation and re-advection of air pollutants, including O_3, in the lower atmosphere. Both the low wind speed during mid-day and its associated recirculation of the O_3 laden air mass by the LSB were successfully simulated and confirmed the accelerated higher O_3 concentrations over the coastal region of the BMA in Korea.

This air quality study pertains to the local circulation interacting with the mesoscale wind patterns, in association with the characteristics of O_3 concentration distributions derived from obser-vational and numerical studies over the BMA. However, further insight into multiple mesoscale wind patterns and their correlation with ambient air quality will be required to confirm the findings presented in this study.

References

Abbs, D.J., Physick, W.L., 1992. Sea-breeze observations and modeling: a review. Australian Meteorological Magazine 41, 7–19.

Bechtold, P., Rinty, J., Mascart, P., 1991. A numerical investigation of the influence of large-scale winds on sea-breeze and inland-breeze-type circulations. Journal of Applied Meteorology 30, 1268–1279.

Blumenthal, D.L., White, W.H., Smith, T.B., 1978. Anatomy of a Los Angles smog episode: pollutant transport in the daytime sea breeze regime. Atmospheric Environment 12, 893–907.

BMC (Busan Metropolitan City), 2002. Report of the improvement of atmospheric environment in Busan metropolitan city. Busan.

Boucouvala, D., Bornstein, R., Wilkinson, J., Miller, D., 2003. MM5 simulations of a SCOS97-NARSTO episode. Atmospheric Environment 37 (Suppl. 2), 95–117.

Chang, M.E., Cardelino, C., 2000. Application of the urban airshed model to forecasting next-day peak ozone concentrations in Atlanta, Georgia. Journal of Air & Waste Management Association 50, 2010–2024.

Ding, A., Wang, T., Zhao, M., Wang, T., Li, Z., 2004. Simulation of sea-breezes and a discussion of their implications on the transport of air pollution during a multi-day ozone episode in the Pearl River Delta of China. Atmospheric Environment 38, 6737–6750.

Dudhia, J., Gill, D., Manning, K., Wang, W., Bruyere, C., 2004. PSU/NCAR Mesoscale Modeling System Tutorial Class Notes and User's Guide MM5 Modeling System Version 3. Mesoscale and Microscale Meteorology Division, National Center for Atmospheric Research.

Helmis, C.G., Papadopoulos, K.H., Kalogiros, J.A., Soilemes, A.T., Asimakopoulos, D.N., 1995. Influence of background flow on evolution of Saronic Gulf sea breeze. Atmospheric Environment 29, 3689–3701.

Hurley, P.J., Manins, P.C., 1995. Meteorological modeling on high-ozone days in Perth, Western Australia. Journal of Applied Meteorology 34, 1643–1652.

Kallos, G., Kassomenos, P., Pielke, R.A., 1993. Synoptic and mesoscale weather conditions during air pollution episodes in Athens, Greece. Boundary-Layer Meteorology 62, 163–184.

Kikuchi, Y., Arakawa, S., Kimura, F., Shirasaki, K., Nagano, Y., 1981. Numerical study on effects of mountains on the land and sea breeze circulation Kanto District. Journal of Meteorological Society of Japan 59, 723–737.

Kim, Y.K., Oh, I.B., Hwang, M.K., 2003. Numerical simulation of ozone using UAM-V on summer episode in the coastal urban area, Busan. Journal of Korean Society for Atmospheric Environment 19 (1), 1–11.

Lalas, D.P., Asimakopoulos, D.N., Delifiorgi, D.G., Helmis, C.G., 1983. Sea-breeze circulation and photochemical

pollution in Athens, Greece. Atmospheric Environment 17 (9), 1621–1632.

Lalas, D.P., Tombrou-Tsella, M., Petrakis, M., Asimakopoulos, D.N., Helmis, C., 1987. An experimental study of the horizontal and vertical distribution of ozone over Athens. Atmospheric Environment 21 (12), 2681–2693.

Liu, C.M., Liu, S.C., Shen, S.H., 1990. The study of Taipei ozone pollution. Atmospheric Environment 24A, 1461–1472.

Liu, K.Y., Wang, Z., Hsiao, L.F., 2002. A modeling of the sea breeze and its impacts on ozone distribution in northern Taiwan. Environmental Modeling & Software 17, 21–27.

Ma Yimin, Lyons, T.J., 2000. Numerical simulation of a sea breeze under dominant synoptic condition at Perth. Meteorological Atmospheric Physics 73, 89–103.

Ma Yimin, Lyons, T.J., 2003. Recirculation of coastal urban air pollution under a synoptic scale thermal trough in Perth, Western Australia. Atmospheric Environment 37, 443–454.

MOE (Ministry of Environment Republic of Korea), 2003. Environmental Statistics Yearbook–Air Quality Emission, p. 107.

Moussiopoulos, N., Sahm, P., Kessler, CH., 1955. Numerical simulation of photochemical smog formation in Athens, Greece–a case study. Atmospheric Environment 24, 3619–3632.

Oh, I.B., Kim, Y.K., 2002. Surface ozone in the major cities of Korea: trends, diurnal and seasonal variations, and horizontal distributions. Journal of Korean Society for Atmospheric Environment 18 (4), 253–264.

Pielke, R.A., 1974. A three-dimensional numerical model of the sea breezes over south Florida. Monthly Weather Review 102, 115–139.

Pielke, R.A., 2002. Mesoscale Meteorological Modeling. Academic Press, New York, p. 474.

SAI (Systems Applications International), 1999. User's Guide to the Variable-Grid Urban Airshed Model (UAM-V), Systems Applications International Inc. (SYSAPP-99-95/27r2).

Simpson, J.E., 1994. Sea Breeze and Local Winds. Cambrige University Press, Cambrige, p. 7.

Uno, I., Wakamatsu, S., Suzuki, M., Ogawa, Y., 1984. Three-dimensional behavior of photochemical pollutants covering the Tokyo metropolitan area. Atmospheric Environment 18 (4), 751–761.

US EPA (United States Environmental Protection Agency), 1991. Guideline for Regulatory Application of the Urban Airshed Model. EPA-450/4-91-013, July 1991, US EPA, Research Triangle Park, NC 27711.

Wakamatsu, S., Uno, I., Ohara, T., Schere, K.L., 1999. A study of the relationship between photochemical ozone and its precursor emissions of nitrogen oxides and hydrocarbons in Tokyo and surrounding areas. Atmospheric Environment 33, 3097–3108.

Wang, T., Lam, K.S., Lee, A.S.Y., Pang, S.W., Tsui, W., 1998. Meteorological and chemical characteristics of the photochemical ozone episodes observed at Cape D'Aguilar in Hong Kong. Journal of Applied Meteorology 37, 1167–1178.

Wang, T., Wu, Y.Y., Cheung, T.F., Lam, K.S., 2001. A study of surface ozone and the relation to complex wind flow in Hong Kong. Atmospheric Environment 35, 3203–3215.

Zhong, S., Takle, E.S., 1993. The effects of large-scale winds on the sea–land-breeze circulations in an area of complex coastal heating. Journal of Applied Meteorology 32, 1181–1195.